J|A|C|S
ARTICLES
Published on Web 08/24/2004

Chelating Ligands for Nanocrystals' Surface Functionalization

Claudia Querner,[†] Peter Reiss,*[,†] Joël Bleuse,[‡] and Adam Pron[†]

Contribution from Service des Interfaces et des Matériaux Moléculaires et Macromoléculaires, Laboratoire Physique des Métaux Synthétiques, and Service de Physique des Matériaux et des Microstructures, Laboratoire Physique des Semi-Conducteurs, Département de Recherche Fondamentale sur la Matière Condensée, CEA Grenoble, 17 rue des Martyrs, 38054 Grenoble Cedex 9, France

Received March 30, 2004; E-mail: preiss@cea.fr

Abstract: A new family of ligands for the surface functionalization of CdSe nanocrystals is proposed, namely alkyl or aryl derivatives of carbodithioic acids (R−C(S)SH). The main advantages of these new ligands are as follows: they nearly quantitatively exchange the initial surface ligands (TOPO) in very mild conditions; they significantly improve the resistance of nanocrystals against photooxidation because of their ability of strong chelate-type binding to metal atoms; their relatively simple preparation via Grignard intermediates facilitates the development of new bifunctional ligands containing, in addition to the anchoring carbodithioate group, a second function, which enables the grafting of molecules or macromolecules of interest on the nanocrystal surface. To give an example of this approach, we report, for the first time, the grafting of an electroactive oligomer from the polyaniline family—aniline tetramer—on CdSe nanocrystals after their functionalization with 4-formyldithiobenzoic acid. The grafting proceeds via a condensation reaction between the aldehyde group of the ligand and the terminal primary amine group of the tetramer. The resulting organic/inorganic hybrid exhibits complete extinction of the fluorescence of its constituents, indicating efficient charge or energy transfer between the organic and the inorganic semiconductors.

Introduction

Research on semiconductor nanocrystals is a field of steadily growing interest due to their unique photophysical properties[1] and to their high potential for substituting traditional compounds in various domains such as optoelectronics[2] or biological labeling.[3] A key issue for many of these applications is the control of the nanocrystals' surface chemistry. As the number of surface atoms depends on the inverse of the diameter, for sizes below ca. 2 nm more than half of the atoms are located on the nanocrystal surface, dominating a large number of its properties. In contrast to core atoms, the coordination sphere of surface atoms is not complete. This gives rise to the formation of dangling bonds, which, among others, can act as traps for photogenerated charge carriers and decrease the nanocrystals' emission efficiency. By proper passivation of these surface trap states, the photoluminescence quantum yield (QY) of CdSe nanocrystals can be improved by more than 1 order of magnitude. This has been achieved by growing an epitaxial-type shell of a second, larger band-gap semiconductor such as ZnS,[4] ZnSe,[5] or CdS[6] on the CdSe surface. On the other hand, the question of surface chemistry remains essentially unchanged, being now associated with the shell surface.

From a chemist's standpoint, the nature of the ligand being coordinated to the nanocrystal surface, and in particular the type of bonds which it forms with the nanocrystal surface atoms, is of crucial importance. Via ligand design, several important properties of the nanocrystals can be tuned, such as their processibility, reactivity, and stability, with direct consequences on their spectroscopic properties. Nevertheless, relatively few literature examples exist concerning the conception of new types of nanocrystal surface ligands. Among them, recently developed oligomeric phosphines[7] and thiol dendrimers[8] should be mentioned.

Three principal functions of the surface ligands can be briefly described as follows: (1) They prevent individual colloidal nanocrystals from aggregation. (2) They facilitate nanocrystals' dispersion in a large variety of solvents. In the presence of surface ligands, the ability to disperse nanocrystals is governed by the difference between the ligand and the solvent solubility

[†] Service des Interfaces et des Matériaux Moléculaires et Macromoléculaires, Laboratoire Physique des Métaux Synthétiques.

[‡] Service de Physique des Matériaux et des Microstructures, Laboratoire Physique des Semi-Conducteurs.

(1) Woggon, U. *Optical Properties of Semiconductor Quantum Dots*; Springer: New York, 1997.
(2) (a) Coe, S.; Woo, W.-K.; Bawendi, M. G.; Bulovic, V. *Nature* **2002**, *420*, 800−803. (b) Huynh, W. U.; Dittmer, J. J.; Alivisatos, A. P. *Science* **2002**, *295*, 2425−2427.
(3) (a) Bruchez, M.; Moronne, M.; Gin, P.; Weiss, S.; Alivisatos, A. P. *Science* **1998**, *281*, 2013−2016. (b) Chan, W. C. W.; Nie, S. M. *Science* **1998**, *281*, 2016−2018. (c) Mattoussi, H.; Mauro, J. M.; Goldman, E. R.; Anderson, G. P.; Sundar, V. C.; Mikulec, F. V.; Bawendi, M. G. *J. Am. Chem. Soc*. **2000**, *122*, 12142−12150.
(4) (a) Guyot-Sionnest, P.; Hines, M. A. *J. Phys. Chem.* **1996**, *100*, 468−471. (b) Daboussi, O.; Rodriguez-Viejo, J.; Mikulec, F. V.; Heine, J. R.; Mattoussi, H.; Ober, R.; Jensen, K. F.; Bawendi, M. G. *J. Phys. Chem. B* **1997**, *101*, 9463−9475.
(5) Reiss, P.; Bleuse, J.; Pron, A. *Nano Lett.* **2002**, *2*, 781−784.
(6) Peng, X.; Schlamp, M. C.; Kadavanich, A. V.; Alivisatos, A. P. *J. Am. Chem. Soc.* **1997**, *119*, 7019−7029.
(7) Kim, S.; Bawendi, M. G. *J. Am. Chem. Soc.* **2003**, *125*, 14652−14653.
(8) (a) Wang, Y. A.; Li, J. J.; Chen, H. Y.; Peng, X. *J. Am. Chem. Soc.* **2002**, *124*, 2293−2298. (b) Guo, W. H.; Li, J. J.; Wang, Y. A.; Peng, X. *J. Am. Chem. Soc*. **2003**, *125*, 3901−3909.

10.1021/ja047882c CCC: $27.50

parameters, which can be precisely tuned. In view of nanocrystals' applications in biological labeling, ligands enabling their dispersion in aqueous solutions are of special interest. (3) Ligands containing appropriate functional groups may serve as "bridging" units for the coupling of molecules or macromolecules to nanocrystals or their grafting on substrates. Thus, appropriate ligand design opens up the possibility of fabrication of new nanocrystal-based organic/inorganic hybrid materials.

In a typical nanocrystals' synthesis, ligands preventing their aggregation are present in the reaction medium. Depending on the intended application, these "original" ligands must be replaced by new ones, which introduce the desired solubility and/or functionality. For this purpose, bifunctional ligands X−Y−Z are frequently used, in which X is a chemical function with a high affinity for the nanocrystal surface, Y is a spacer of alkyl or aryl type, and Z is the group transferring the desired property to the nanocrystal. The main advantages of this approach are the well-defined surface chemistry of the nanocrystals after functionalization and the possibility to maintain essentially their original size. In most literature examples, the function X stands for one or two thiol groups.[3,9] This preference can be partially attributed to the large commercial availability of thiols with numerous spacers Y and functional groups Z. Although convenient in use, thiol-based ligands show however some weaker points. For example, photodegradation studies reveal that thiols coordinated on CdSe nanocrystals readily undergo photooxidation accompanied by the formation of disulfides, which leads to the precipitation of the crystals.[10] This photochemical instability can be ascribed to the relatively weak interaction between the nanocrystal surface and the thiol ligand, which is not of a covalent nature. Furthermore, quasi-quantitative substitution (>95%) of the original surface ligands (e.g. TOPO) by thiols requires usually extended exchange reaction times and can be achieved only in relatively drastic reaction conditions[11] which, in turn, might affect other properties of the nanocrystals, such as their QY.

These shortcomings motivated us to develop a new type of bifunctional ligands, which contain a carbodithioate ($-C(S)S^-$) function serving as the anchor group for the nanocrystal surface. Several features make them attractive candidates for nanocrystal functionalization. Their high affinity for metal atoms, which arises from the bidentate chelating binding of the carbodithioate group, facilitates the replacement of the original surface ligands. Quasi-quantitative exchange is achieved in a room-temperature reaction within 1−3 h. In addition, nanocrystals capped with the carbodithioate ligands exhibit a significantly enhanced stability against photodegradation with respect to the corresponding thiol ligands. Finally, the new ligands can be easily synthesized via a Grignard reaction. The simplicity and generality of the proposed synthetic approach open up the possibility of the preparation of "tailor-made" molecules. This is illustrated here by the synthesis of a ligand which has been designed for the grafting of electroactive molecules (aniline tetramers) on the nanocrystal surface, resulting in a new organic/inorganic hybrid compound with potential interest for use in photovoltaic devices.

Experimental Section

Chemicals. Anhydrous solvents and all reagents (Aldrich) were of the highest purity available. Trioctylphosphine (TOP, 90%) and hexadecylamine (HDA, 90%) were additionally purified by distillation.

Characterization Techniques. All synthesized precursors and ligands were identified by ^{1}H and ^{13}C NMR spectroscopy on a Bruker AC 200-MHz spectrometer; acetone-d_6, chloroform-d, and DMSO-d_6 containing TMS as internal standard were used as solvents according to the solubility of the product. The purity of the synthesized molecules was verified by elemental analysis (Analytical Service of CNRS Vernaison, France). FT-IR spectra were recorded on a Perkin-Elmer Paragon500 spectrometer (wavenumber range 4000−400 cm^{-1}; resolution 2 cm^{-1}) using the ATR technique. Solution UV−vis spectra were recorded on a Hewlett Packard 8452A spectrometer (wavelength range 180−820 nm). Photoluminescence spectroscopy investigations were carried out on a Jobin-Yvon HR 550 monochromator equipped with a CCD silicon detector cooled at 140 K. Excitation was performed with an argon laser at 365 nm or with a blue, 400-nm LED.

Synthesis of CdSe Nanocrystals. The synthetic procedure used in this research for the preparation of CdSe core nanocrystals has been described in ref 5, using a molar ratio of 70% HDA in the TOPO/HDA solvent mixture. The obtained TOPO-capped CdSe nanocrystals had an average diameter of 4.2 nm (determined by TEM).

^{1}H NMR ($CDCl_3$, 200 MHz): δ 1.7−1.4 (s, 6H), 1.19 (s, 36H), 0.81 (s, 9H). UV−vis ($CHCl_3$): λ = 561 nm (excitonic peak), 460 nm (higher excited state). PL ($CHCl_3$): 575 nm.

General Procedure for the Synthesis of Carbodithioic Acids. The preparation consists of a Grignard reaction of alkyl- or arylmagnesium bromides with carbon disulfide (CS_2), based on procedures described in the literature.[12] **Caution: Carbon disulfide is highly toxic and has to be handled under a fume hood or in a drybox.** Dried magnesium turnings (5 equiv) were covered with anhydrous THF in a round-bottom flask under argon flux. A solution of alkyl- or arylbromine (1 equiv) dissolved in anhydrous THF was added dropwise. The resulting mixture was vigorously stirred under reflux for 2 h. The colored solution was then cooled and transferred via cannula to a flask containing carbon disulfide (3 equiv) in anhydrous THF, previously cooled to −5 to 0 °C. After addition, the reaction mixture was allowed to warm to room temperature and left overnight with constant stirring. In the next step, the product was hydrolyzed with a 1:1 diethyl ether:water mixture. The aqueous layer was then acidified using 0.2 M HCl and extracted with diethyl ether. The organic layer was repeatedly washed with water, dried over $MgSO_4$, and concentrated using a rotary evaporator.

Tridecanedithioic Acid (1). A 3.46-g yield of a yellow, partially crystallized product was obtained from 5 g of *n*-bromododecane (70% yield), using the procedure described above.

^{1}H NMR ($CDCl_3$, 200 MHz): δ 2.99 (t, 2H, J = 6.7 Hz), 1.78 (q, 2H, J = 6.7 Hz), 1.4−1.0 (m, 18H), 0.81 (t, 3H, J = 6.7 Hz); S-**H** is not visible. ^{13}C NMR ($CDCl_3$, 200 MHz): δ 14.02, 22.64, 28.57, 29.17, 29.31, 29.40, 29.57 (2C), 29.64 (2C), 31.87, 52.89, 238.76. Elemental analysis calculated for $C_{13}H_{26}S_2$: C, 63.35; H, 10.63; S, 26.02. Found: C, 62.88; H, 10.52; S, 25.17. UV−vis ($CHCl_3$): λ_{max} = 300 nm.

4-Methyldithiobenzoic Acid (2). A 0.72-g yield of a violet solid was obtained from 1.7 g of 4-bromotoluene (43% yield), using the procedure described above. This crude product was then purified by recrystallization in MeOH.

^{1}H NMR ($CDCl_3$, 200 MHz): δ 7.89 (d, 2H, J = 8.3 Hz), 7.10 (d, 2H, J = 8.3 Hz), 6.20 (S-**H**, s, 1H), 2.30 (s, 3H). ^{13}C NMR ($CDCl_3$,

(9) (a) Pathak, S.; Choi, S. K.; Arnheim, N.; Thompson, M. E. *J. Am. Chem. Soc.* **2001**, *123*, 4103−4106. (b) Wuister, S. F.; Swart, I.; van Driel, F.; Hickey, S. G.; de Mello Donega, C. *Nano Lett.* **2003**, *3*, 503−507.
(10) Aldana, J.; Wang, Y. A.; Peng, X. *J. Am. Chem. Soc.* **2001**, *123*, 8844−8850.
(11) (a) Kuno, M.; Lee, J. K.; Dabbousi, B. O.; Mikulec, F. V.; Bawendi, M. G. *J. Chem. Phys.* **1997**, *106*, 9869−9882. (b) Peng, X.; Wilson, T. E.; Alivisatos, A. P.; Schultz, P. G. *Angew. Chem., Int. Ed. Engl.* **1997**, *36*, 145−147.
(12) (a) Houben, J.; Kesselkaul, L. *Ber. Dtsch. Chem. Ges.* **1902**, *35*, 3695−3699. (b) Houben, J.; Pohl, H. *Ber. Dtsch. Chem. Ges.* **1907**, *40*, 1725−1730. (c) Ramadas, S. R.; Srinivasan, P. S.; Ramachandran, J.; Sastry, V. V. S. K. *Synthesis* **1983**, 605−622. (d) Colorado, R., Jr.; Villazana, R. J.; Lee, T. R. *Langmuir* **1998**, *14*, 6337−6340.

200 MHz): δ 21.52, 126.91 (2C), 129.00 (2C), 140.96, 144.46, 224.55. Elemental analysis calculated for $C_8H_8S_2$: C, 57.10; H, 4.79; S, 38.11. Found: C, 57.00; H, 4.87; S, 37.70. UV−vis ($CHCl_3$): λ_{max} = 315 nm.

4-Formyldithiobenzoic Acid (5). 4-Bromobenzaldehyde (1.93 g, 10 mmol) and 2,2-dimethyl-1,3-propanediol (10.88 g, 100 mmol) were dissolved in 60 mL of toluene in a round-bottom flask. Trifluoroacetic acid (0.25 mL, 3×10^{-3} mmol) was then added, and the mixture was heated at 90 °C for 15 h. In the next step, the reaction mixture was washed with a saturated solution of K_2CO_3 and then with water. The organic layer was concentrated, and the product was recrystallized in water to give 2.63 g (94% yield) of 2-(4-bromophenyl)-5,5-dimethyl-1,3-dioxane (**3**) (white solid).

^{1}H NMR ($CDCl_3$, 200 MHz): δ 7.43 (dd, 2H, J = 8.8 Hz, 2.2 Hz), 7.31 (dd, 2H, J = 8.8 Hz, 2.2 Hz), 5.27 (s, 1H), 3.63 (dd, 4H, J = 26 Hz, 11 Hz), 1.20 (s, 3H), 0.73 (s, 3H). ^{13}C NMR ($CDCl_3$, 200 MHz): δ 21.83, 23.00, 30.18, 77.62 (2C), 100.92, 122.84, 127.93 (2C), 131.37 (2C), 137.58. Elemental analysis calculated for $C_{12}H_{15}BrO_2$: C, 53.16; H, 5.58; Br, 29.47; O, 11.80. Found: C, 52.93; H, 5.57.

From 4.12 g of **3**, 2.12 g of 4-(5,5-dimethyl-1,3-dioxan-2-yl)-dithiobenzoic acid (**4**) was obtained (62% yield) using the general procedure described above. The product in the form of a violet solid was recrystallized in methanol.

^{1}H NMR ($CDCl_3$, 200 MHz): δ 8.04 (dd, 2H, J = 8.4 Hz, 2.2 Hz), 7.53 (dd, 2H, J = 8.4 Hz), 6.38 (S-**H**, s, 1H), 5.41 (s, 1H), 3.72 (dd, 4H, J = 26 Hz, 11 Hz), 1.28 (s, 3H), 0.81 (s, 3H). ^{13}C NMR ($CDCl_3$, 200 MHz): δ 21.87, 23.01, 30.29, 77.66 (2C), 100.67, 126.23 (2C), 126.80 (2C), 143.38, 143.65, 224.95. Elemental analysis calculated for $C_{13}H_{16}O_2S_2$: C, 58.17; H, 6.01; S, 23.89; O, 11.92. Found: C, 58.10; H, 6.06; S, 23.86. UV−vis ($CHCl_3$): λ_{max} = 305 nm.

One milliliter of H_2O and 10 mL of concentrated CF_3COOH were added to a solution of **4** (205 mg, 0.76 mmol) in 2 mL of $CHCl_3$. The solution was stirred at room temperature for 4 h. The reaction mixture was then diluted with 10 mL of $CHCl_3$ and neutralized with a saturated aqueous solution of K_2CO_3. 4-Formyldithiobenzoic acid (**5**) was obtained either in its potassium salt form (**5′**) (yellow-orange solid after extraction from the aqueous layer) or as the free acid **5** (dark-red solid, 85 mg, 61%) by acidifying with 0.2 M HCl.

(a) Characterization of the Free Acid 5. ^{1}H NMR ($CDCl_3$, 200 MHz): δ 10.01 (s, 1H), 7.92 (d, 2H, J = 8.6 Hz), 7.85 (d, 2H, J = 8.6 Hz), 6.35 (S-**H**, s, 1H). ^{13}C NMR ($CDCl_3$, 200 MHz): δ 129.67 (2C), 130.04 (2C), 191.19, 228.86. Elemental analysis calculated for $C_8H_6OS_2$: C, 52.71; H, 3.32; O, 8.78; S, 35.17. Found: C, 52.91; H, 3.39; S, 33.74.

(b) Characterization of the Potassium Salt 5′. ^{1}H NMR (acetone-d_6, 200 MHz): δ 10.03 (s, 1H), 8.32 (d, 2H, J = 8.4 Hz), 7.72 (d, 2H, J = 8.6 Hz). ^{13}C NMR (acetone-d_6, 200 MHz): δ 128.76 (2C), 129.71 (2C), 137.34, 193.75, 252.80. Elemental analysis calculated for $C_8H_5OS_2K$: C, 43.60; H, 2.29; K, 17.74; O, 7.26; S, 29.10. Found: C, 43.15; H, 2.66; S, 28.67.

Aniline tetramer in the oxidation state of emeraldine (6) was prepared using a modification of the method described in ref 13. The exact preparation procedure used in this research can be found elsewhere.[14]

^{1}H NMR (DMSO-d_6, 200 MHz): δ 8.37 (N-**H**, s, 1H), 7.23 (d, 2H, J = 7 Hz), 7.11 (d, 4H, J = 5 Hz), 7.0−6.7 (m, 9H), 6.62 (d, 2H, J = 8 Hz), 5.51 (N-**H**$_2$, s, 2H). UV−vis (DMSO): λ_{max} = 306 nm, λ = 591 nm. IR: ν (cm^{-1}) 1597 (s), 1497 (s), 1320 (m), 1166 (w), 839 (m), 745 (m), 692 (w).

Spectroscopic studies as well as elemental analysis are consistent with the presence of one water molecule per tetramer unit. Elemental analysis calculated for $C_{24}H_{20}N_4 \cdot 1H_2O$: C, 75.20; H, 5.78; N, 14.61; O, 4.41. Found: C, 75.86; H, 5.25; N, 14.54. MS-ESI (H^+ mode): m/z calcd = 364.17, mH$^+$/z found = 365.30.

Model Compound 7. A solution of **6** (18 mg, 0.05 mmol) in 10 mL of anhydrous ethanol was added dropwise to the solution of *p*-bromobenzaldehyde (9 mg, 0.05 mmol) in 5 mL of the same solvent. The mixture was heated overnight under reflux. The precipitate was filtered under an inert atmosphere and washed with a large excess of methanol, then with chloroform, and finally dried in a vacuum to give a black solid (20 mg, 80% yield). ^{1}H NMR (DMSO-d_6, 200 MHz): δ 7.99 (s, 6H), 7.2−6.6 (m, 17H). UV−vis (DMSO): λ_{max} = 325 nm, λ = 618 nm.

General Procedure of Ligand Exchange. A solution of the ligand (thiol or carbodithioic acid, 20 mg in 1 mL of $CHCl_3$) was added to the colloidal solution of CdSe nanocrystals (10 mg in 1 mL of $CHCl_3$). The obtained mixture was then stirred at constant temperature. In the case of carbodithioic acids, the ligand exchange carried out at room temperature for 1−3 h led to a nearly quantitative replacement of the initial surface ligands, as confirmed by ^{1}H NMR. For thiols, the same procedure required strirring at 40 °C for periods up to 3 days. The nanocrystals coated with the new ligands were purified by two cycles of precipitation with methanol and dispersion in chloroform. After being dried under vacuum, they could readily be redispersed in chloroform. Using the above-outlined procedures, CdSe nanocrystals functionalized with dodecanethiol **(Alk-SH)**, tridecanedithioic acid (**1**), 4-methoxybenzenethiol **(Ar-SH)**, 4-methyldithiobenzoic acid (**2**), and 4-(5,5-dimethyl-1,3-dioxan-2-yl)dithiobenzoic acid (**4**) were prepared.

CdSe-Alk-SH (40 °C, 3 days). ^{1}H NMR ($CDCl_3$, 200 MHz): δ 1.6−1.4 (s, 2H), 1.4−1.0 (s, 18.7H), 1.0−0.6 (s, 3H) (15% of the initial TOPO content remained unexchanged). UV−vis ($CHCl_3$): λ = 561 nm (excitonic peak), λ = 460 nm (higher excited state).

CdSe-1 (25 °C, 1 h). ^{1}H NMR ($CDCl_3$, 200 MHz): δ 3.0−2.8 (s, 2H), 1.6−1.4 (s, 2H), 1.4−1.0 (s, 17.4H), 1.0−0.6 (s, 3H) (10% of the initial TOPO content remained unexchanged). UV−vis ($CHCl_3$): λ = 578 nm (excitonic peak), λ = 470 nm (higher excited state).

CdSe-Ar-SH (25 °C, 3 days). ^{1}H NMR ($CDCl_3$, 200 MHz): δ 7.33 (d, 2H, J = 8.8 Hz), 6.77 (d, 2H, J = 8.8 Hz), 3.71 (s, 3H), 1.6−1.4 (s, 25H), 1.4−1.0 (s, 120H), 1.0−0.6 (s, 38H) (70% of the initial TOPO content remained unexchanged). UV−vis ($CHCl_3$): λ = 557 nm (excitonic peak), λ = 457 nm (higher excited state).

CdSe-2 (25 °C, 2 h). ^{1}H NMR ($CDCl_3$, 200 MHz): δ 7.96 (d, 2H, J = 8.3 Hz), 7.17 (d, 2H, J = 8.3 Hz), 2.34 (s, 3H), 1.6−1.4 (s, 0.2H), 1.4−1.0 (s, 1.2H), 1.0−0.6 (s, 0.3H) (<5% of the initial TOPO content remained unexchanged). UV−vis ($CHCl_3$): λ = 323 nm (ligand $\pi-\pi^*$ transition).

Complexation of Cd^{2+} Ions with 2. A 19-mg sample of $CdCl_2$ (0.1 mmol) was suspended in a solution of **2** (34 mg, 0.2 mmol) in 2 mL of $CHCl_3$ and stirred at room temperature. Within 2 h a homogeneous solution formed. UV−vis ($CHCl_3$): λ_{max} = 317 nm.

Grafting of Aniline Tetramer on CdSe Nanocrystals. The procedure consisted of two steps: first, original TOPO ligands were exchanged with potassium 4-formyldithiobenzoate (**5′**) to give aldehyde-capped nanocrystals on which, in a second step, aniline tetramer was grafted (Scheme 1).

(a) Ligand Exchange. Ligand **5′** (12 mg, 0.055 mmol) was placed under an inert atmosphere in a round-bottom flask and dissolved in 10 mL of ethanol. CdSe nanocrystals (10 mg) (0.2 mL of a 50 mg/mL $CHCl_3$ solution) in 10 mL of chloroform were then added, and the mixture was stirred for 2 h at room temperature to give **CdSe-5′**. No intermediate purification was carried out.

(b) Aniline Tetramer Grafting. A solution of **6** (50 mg, 0.136 mmol) in 10 mL of ethanol was added dropwise to the solution of aldehyde-functionalized nanocrystals **CdSe-5′**. The mixture was refluxed overnight under an inert atmosphere. The formed black precipitate was then filtered and washed repeatedly first with methanol, to extract nonreacted tetramer, and then with chloroform, with the goal

(13) Feng, J.; Zhang, W.; MacDiarmid, A. G.; Epstein, A. P. *Proc. Soc. Plast. Eng., Annu. Technol. Conf. (ANTEC97)* **1997**, *2*, 1373−1377.
(14) Dufour, B.; Rannou, P.; Travers, J. P.; Pron, A.; Zagorska, M.; Korc, G.; Kulszewicz-Bajer, I.; Quillard, S.; Lefrant, S. *Macromolecules* **2002**, *35*, 6112−6120.

Scheme 1. Chemical Structures of the Bifunctional Ligand **5**, Grafted and Nongrafted Aniline Tetramer Derivatives, and Their Synthetic Pathways[a]

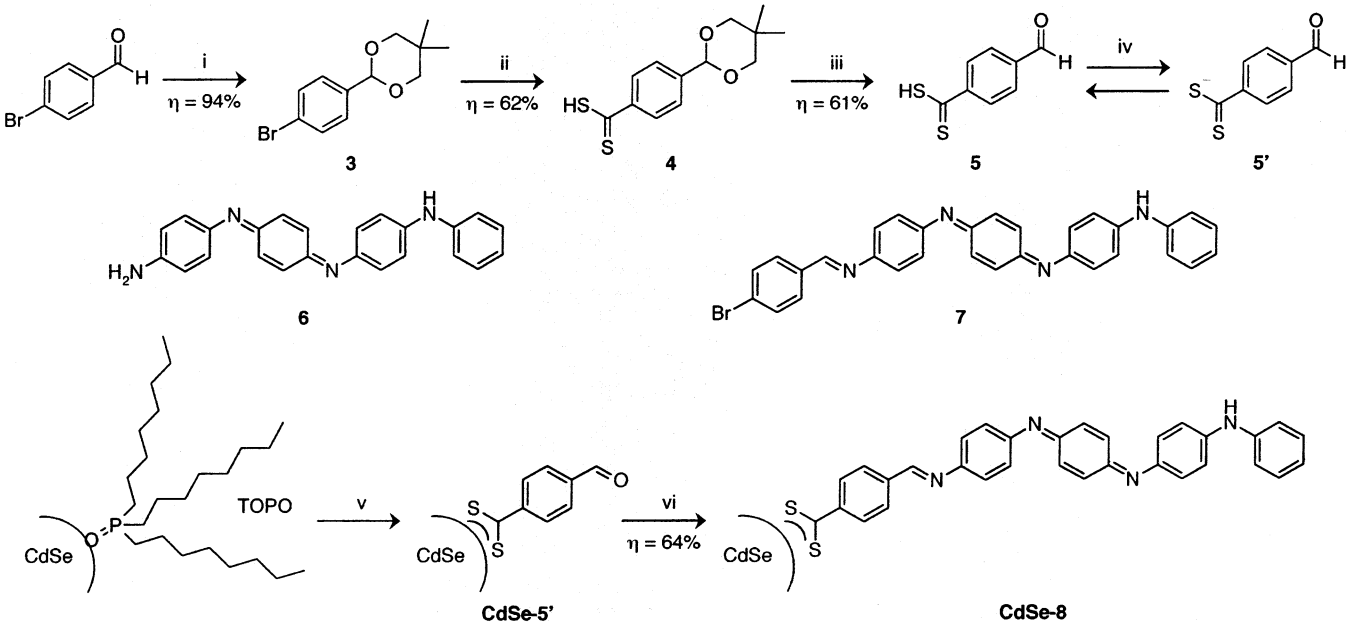

[a] Reagents and conditions: (i) neopentyl glycol, CF_3COOH, toluene, 90 °C; (ii) Mg, THF, 60 °C; CS_2, THF, 0 °C; 2 M HCl; (iii) $CHCl_3$:H_2O:CF_3COOH (2:1:10), 25 °C; (iv) K_2CO_3, 25 °C; (v) **5′**, $CHCl_3$:EtOH (1:1), 25 °C; (vi) **6**, EtOH, 80 °C.

to remove nongrafted aldehyde ligand. The final black solid, **CdSe-8** (7 mg, 64% yield), which consists of aniline-tetramer-functionalized CdSe nanocrystals, is soluble in DMSO or NMP.

^{1}H NMR (DMSO-d_6, 200 MHz): δ 7.99 (s, 6H), 7.2−6.6 (m, 17H). UV−vis (DMSO): λ_{max} = 325 nm, λ = 618 nm. IR: ν (cm^{-1}) 1697 (w), 1597 (s), 1504 (vs), 1297 (s), 1166 (m), 1012 (w) (Ar−CS_2^-), 819 (m), 750 (m), 696 (w).

Photostability Investigations. Colloidal solutions of tridecanedithioate-capped CdSe (**CdSe-1**) and dodecanethiol-capped CdSe nanocrystals (**CdSe-Alk-SH**) in chloroform were placed in quartz cells of 1-mm path length (sample volume 0.3 mL) and purged with air. Their concentrations were adjusted by dilution to be identical for comparative studies, with the absorbance being in the range 0.1−0.3 for the first exciton absorption peak. Photooxidation experiments were carried out by continuous irradiation with an UV lamp (254 or 365 nm, 25 W), placed at a distance of 5 cm from the sample, and recording the UV−vis spectra of the samples in regular intervals.

Results and Discussion

Ligands containing the carbodithioic acid group and their salts have been known for more than one century for their ability to strongly complex metal ions. Their most important literature examples are dithiocarbamates (RR′N−C(S)S^-) and xanthates (RO−C(S)S^-).[15] A common disadvantage of these molecules, in view of a homogeneous exchange reaction with nanocrystals' surface ligands, is the fact that they are—in their salt form—only soluble in water and not in the same solvent as TOPO-capped nanocrystals, used in this research. On the other hand, they generally decompose in acidic conditions, making it difficult to prepare their free acid form, which is usually soluble in organic solvents. As a consequence, we were not able to perform efficient ligand exchange with dithiocarbamates or xanthates. We found, however, that in the case of alkyl- and arylcarbodithioic acids, which are much less studied to date, the lack of a heteroatom in the vicinity of the −C(S)SH group prevents them from decomposition and their acidic forms are stable under an inert atmosphere.

Ligand Exchange. Different exchange procedures can be found in the literature. In the simplest way, nanocrystals containing initial surface ligands are brought into contact with a large excess of the new ligand, which serves as a solvent for nanocrystals' dispersion.[3b] Alternatively, the ligand can be dissolved in an organic cosolvent[9b] or nonsolvent for the nanocrystals.[9a,11b] If used as the solvent, the new ligand must be a liquid at the temperature of the exchange reaction; moreover, a relatively high quantity of the ligand molecules is required. This is a significant drawback when expensive or tailor-made compounds are to be used, since the excess of the new ligand is usually discarded during purification steps. For this reason, here the second procedure was applied. The synthesized ligands were dissolved in chloroform, which is also a cosolvent for nanocrystals containing TOPO surface ligands—and, importantly, also for free TOPO. An approximately 10-fold excess of the carbodithioate or thiol ligand with respect to the calculated molar quantity of surface TOPO molecules was used.[16] This homogeneous reaction leads to nearly quantitative exchange with TOPO for the alkyl- or arylcarbodithioate ligands at room temperature and for the corresponding thiols at 40 °C. The functionalized nanocrystals are then purified by precipitation and washing with MeOH.

The degree of surface ligand exchange can be controlled by ^{1}H NMR spectroscopy if appropriate diagnostic peaks are selected. TOPO-capped CdSe nanocrystals exhibit characteristic peaks of alkyl chains with chemicals shifts in the range of 0.5−1.5 ppm. In 4-methoxybenzenethiol-capped CdSe (**CdSe-Ar-SH**), the methoxy group gives rise to a peak at 3.7 ppm, and finally 4-methyldithiobenzoate-capped CdSe (**CdSe-2**) can be identified by its methyl protons at 2.3 ppm.

(15) For reviews, see: (a) Coucouvanis, D. *Prog. Inorg. Chem.* **1970**, *11*, 233−371. (b) Eisenberg, R. *Prog. Inorg. Chem.* **1971**, *12*, 295−369.

(16) Striolo, A.; Ward, J.; Prausnitz, J. M.; Parak, W. J.; Zanchet, D.; Gerion, D.; Milliron, D.; Alivisatos, A. P. *J. Phys. Chem. B* **2002**, *106*, 5500−5505.

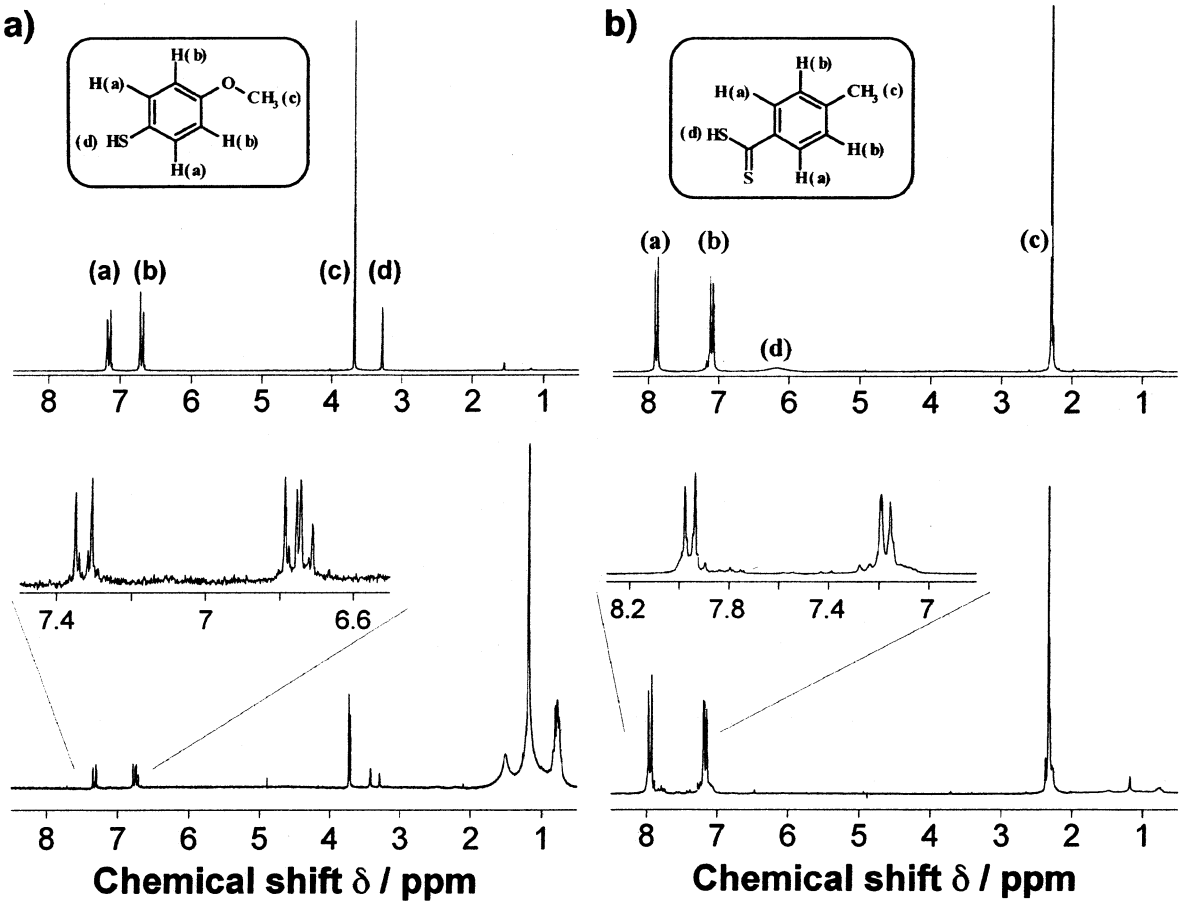

Figure 1. (a) ^{1}H NMR spectra of 4-methoxybenzenethiol (top) and of TOPO-capped CdSe nanocrystals after surface ligand exchange with this compound (bottom, reaction time 72 h at room temperature). (b) ^{1}H NMR spectra of 4-methyldithiobenzoic acid (**2**) (top) and of TOPO-capped nanocrystals after exchange with **2** (bottom) (reaction time 2 h at room temperature).

This separation of the diagnostic peaks facilitates quantitative determination of the degree of ligand exchange.

Such quantitative analysis is, more difficult in the case of aliphatic ligands because chemical shifts ascribed to their protons are very similar to those recorded for the protons of the TOPO alkyl chains. In both cases, however, in the aliphatic part of the spectrum, three relatively well separated groups of lines can be distinguished: the up-field triplet (0.8 ppm) corresponding to the methyl group, the low-field poorly resolved line (1.5 ppm) corresponding to the methylene group adjacent to phosphorus or sulfur, and a poorly resolved multiplet in the mid-field (1.2 ppm), corresponding to the remaining methylene groups. From the ratio of the integrated intensities of the mid-field peak and the up-field peak, the degree of ligand exchange can be estimated because this ratio depends on the mutual TOPO and Alk-SH content. This method was used for the calculation of the exchange degree reported in the Experimental Section (vide supra).

It is clear from ^{1}H NMR data that the use of the newly developed carbodithioate chelating ligands results in a faster and more complete ligand exchange as compared to the corresponding thiol ligands, at least in the mild reaction conditions applied in this research. This indicates a much higher affinity of the anchoring carbodithioate group toward the surface of CdSe nanocrystals. An instructive example of this significant difference in the complexing ability between the carbodithioate and thiol ligands can be provided by analyzing the NMR spectra presented in Figure 1. With the goal of easier line identification, the spectra of the thiol and the carbodithioate-capped nanocrystals are compared with those registered for the free ligands.

At room temperature, the exchange of TOPO by 4-methoxybenzenethiol **(Ar-SH)** is very inefficient, and even after 3 days exchange time approximately 70% of TOPO, as determined by the integration, still remains on the nanocrystal surface (Figure 1a). To the contrary, if 4-methyldithiobenzoic acid (**2**) is used in the exchange reaction, within 2 h almost no TOPO remains on the nanocrystal surface. Integration exhibits that the TOPO content is less than 5% (Figure 1b), which is at the same time the limit of reliable determination by this method. Moreover, it has to be noted that the signal at 6.2 ppm, originating from the proton in the carbodithioic acid group (C(S)S*H*), is absent in the spectrum of **CdSe-2**, revealing that the ligand binds to the nanocrystal surface in its deprotonated form as carbodithioate.

Finally we must notice that the ligand coordination on the nanocrystal surface induces a significant downfield shift of the lines corresponding to all aromatic protons (H_a, H_b, H_c). As expected, this shift, caused by the deshielding effect, is the most pronounced for H_a protons, which are in the closest vicinity of the anchor groups and equal to 0.16 and 0.08 ppm for the thiol and carbodithioate ligands, respectively. With increasing distance from the anchoring group this downfield shift decreases, being the least pronounced for H_c protons. This behavior can be taken as a spectroscopic manifestation of the ligand coordination on the nanocrystal surface.

The NMR lines recorded for the nanocrystal surface ligands are relatively narrow, especially in view of the fact that the ligands' coordination should result in their restricted motion and, as a consequence, in a NMR line broadening. It has been however demonstrated that the coordination of thiophenol ligands on the nanocrystal surface does not result in a significant line broadening because of the possibility of a rotation around the Cd−S bond.[17] This motion is less hindered as the nanocrystal size increases due to a lower coverage of ligands on the surface resulting in a decreasing steric hindrance. Similar or even more pronounced effects are expected for 4-methoxybenzenethiol ligands used in our study, taking into account their chemical similarity to the thiophenol ligand and the relatively large size of the nanocrystals used (diameter 4.2 nm). In the case of carbodithioate ligands, the rotation about the Cd−S bond is hindered because of the chelate-type bonding of these molecules to the nanocrystal surface. Though broader than in the case of the thiol-capped nanocrystals, the observed NMR lines are still relatively narrow, and we are assuming that the carbodithioate ligand molecules are able to rotate around the C−C bond between the anchor group and the phenyl ring.

In the case of carbodithioate ligands containing aryl subsituents, UV−vis spectroscopy is an additional tool to monitor the complexation process since the chelating effect induces spectral changes in the absorption spectrum of the ligand. In particular, it is known that the bidentate coordination of carbodithioates to metal ions (formation of four-membered-ring chelates) results in a bathochromic shift of the band ascribed to the $\pi-\pi^*$ transition in the aromatic ring as compared to the same band in the corresponding carbodithioic acid.[18] The expected, complexation-induced, bathochromic shift is also observed for ligand **2**. Its free acid form gives rise to an absorption band with a maximum at 304 nm. Upon coordination to Cd^{2+} ions, the band shifts to 317 nm. An even more pronounced bathochromic shift is observed after the exchange of TOPO on the nanocrystal surface with ligand **2**, since for **CdSe-2** the $\pi-\pi^*$ transition band is located at 321 nm. This can be considered as an indication of a strong coordination of the ligand in its bidentate chelating form, similar to that observed in mononuclear metal complexes. It should be noted here that, for CdSe nanocrystals capped with carbodithioate ligands containing alkyl or aryl substituents, the ligand proper bands and the nanocrystal excitonic bands are spectrally well separated and do not interfere.

We have also investigated the effect of the ligand exchange process on the photoluminescence (PL) properties of the nanocrystals. For comparative reasons, in Figure 2 the PL spectrum of CdSe capped with the initial surface ligands (**CdSe-TOPO)** is shown together with the spectra of the same nanocrystals after the exchange with tridecanedithioate and dodecanethiol ligands, termed **CdSe-1** and **CdSe-Alk-SH**, respectively. Upon ligand exchange, we first notice a decrease of the PL, which is slightly more pronounced for **CdSe-Alk-SH** (90%) than for **CdSe-1** (85%). In the latter case, this is accompanied by a small bathochromic shift of the PL peak maximum from 577 to 583 nm, while, in the former case, a hypsochromic shift by 6 nm is observed. For both systems studied, the full width at half-maximum (fwhm) of the PL peak remains the same (ca. 35 nm).

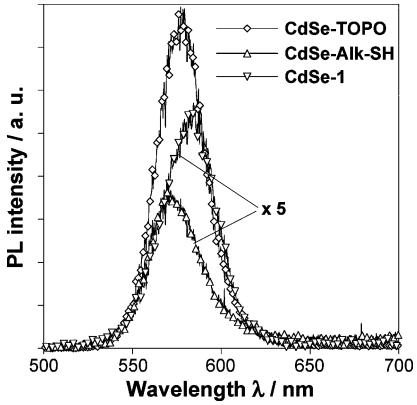

Figure 2. PL spectra of CdSe nanocrystals before and after exchange of the surface TOPO ligands with dodecanethiol (**CdSe-Alk-SH**) and with tridecanedithioate (**CdSe-1**), excited at 400 nm.

Aryl carbodithioate ligands, containing an aromatic ring adjacent to the anchor group, efficiently quench the photoluminescence of nanocrystals. This phenomenon is discussed in detail in the last section of the paper, devoted to CdSe−aniline tetramer organic/inorganic hybrids.

Photostability. Strong coordination of the newly developed ligands on the surface of CdSe nanocrystals may increase considerably their photochemical stability, since appropriate surface passivation should prevent photooxidation or at least significantly slow this process. Poor resistance against photooxidation is frequently one of the weakest points of nanocrystal-based materials, which severely limits their technological applications. Therefore, any improvement in the photochemical stability of CdSe nanocrystals is not only of fundamental but also of practical interest. For this reason we have undertaken the task of comparative investigations of tridecanedithioate-capped CdSe nanocrystals (**CdSe-1**) and dodecanethiol-capped ones (**CdSe-Alk-SH**). We have chosen this set of ligands because thiols containing long alkyl chains have been reported to be the most resistant systems among other thiols in a photooxidation study carried out in water.[10] As the two ligands differ only in the chemical nature of the anchor group, its influence on the photochemical stability of nanocrystals can be selectively investigated. Figure 3 shows the results of photodegradation experiments carried out under continuous monochromatic irradiation ($\lambda = 365$ nm). For $\lambda = 254$ nm similar behavior is observed, although, as expected, the photodegradation is accelerated by the irradiation at higher energy. For comparative reasons the spectra of nanocrystals capped with initial surface ligand (TOPO) are shown in Figure 3a. These nanocrystals are the least UV stable and start precipitating after 9 h of constant irradiation. Simultaneously, an increasing blue shift of the excitonic peak is observed with increasing irradiation time. As can be clearly seen in Figure 3b, for short exposure times (up to 16 h), the thiol-capped nanocrystals show no signs of photodegradation, such as precipitation or blue shift of the excitonic peak. They then start to oxidize, and after ca. 30 h they are totally degraded, which results in their quantitative precipitation. The carbodithioate-capped nanocrystals behave differently (Figure 3c). In this case, a small blue shift of the excitonic peak is observed for irradiation times shorter than 3 h, and then its position stabilizes. The nanocrystals do not precipitate even after 67 h of constant exposure to the UV irradiation. Moreover, their spectral features remain essentially

(17) Sachleben, J. R.; Colvin, V.; Emsley, L.; Wooten, E. W.; Alivisatos, A. P. *J. Phys. Chem. B* **1998**, *102*, 10117−10128.
(18) Furlani, C.; Luciani, M. L. *Inorg. Chem.* **1968**, *7*, 1586−1592.

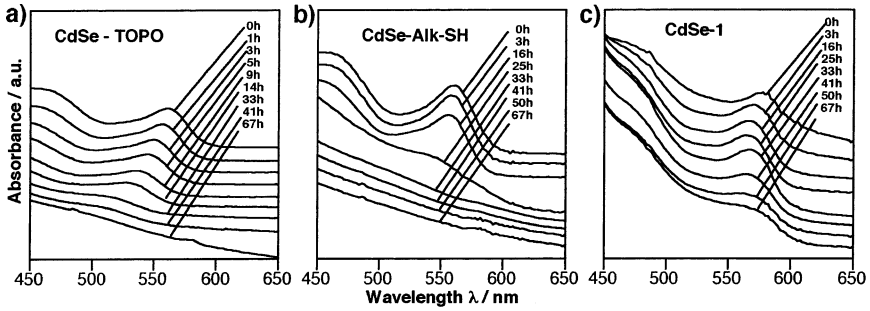

Figure 3. Photostability investigations by UV−vis spectroscopy of (a) TOPO-capped CdSe nanocrystals, (b) after exchange of TOPO with dodecanethiol (**CdSe-Alk-SH**), and (c) after exchange with tridecanecarbodithioic acid (**CdSe-1**). The spectra are taken after the indicated periods of continuous UV irradiation (365 nm); they are vertically shifted for clarity.

unchanged apart from some broadening of the first excitonic peak observed for exposure times exceeding 40 h. The small blue shift of the excitonic peak observed for short exposure times could in principle be considered as a spectroscopic manifestation of the onset of nanocrystals' oxidation. However, taking into account the quick stabilization of the nanocrystals' optical parameters with further irradiation, we are tempted to explain the observed phenomenon by changes in the ligand−nanocrystal interactions rather than as a result of photooxidation. Such interactions can, for example, be modified by irradiation-induced structural rearrangement. Furthermore, it should be noted here that the position of the excitonic peak of **CdSe-1** is red-shifted by 17 nm with respect to that of CdSe-TOPO. The registered irradiation-induced blue shift reverses this behavior by only 7 nm, indicating that it does not originate from the photooxidation of the nanocrystal surface, which should result in a more pronounced and continuous evolution.

Organic/Inorganic Hybrids via Grafting of Aniline Tetramer on Nanocrystals Capped with an Aldehyde-Functionalized Carbodithioate Ligand. The facility of quantitative exchange with TOPO and their good anchoring properties make carbodithioic acids excellent candidates for the preparation of special bifunctional ligands, which could be used for the grafting of organic molecules of interest on semiconductor nanocrystals. The elaboration of such hybrid systems consisting of conjugated oligomers or polymers and nanocrystals is especially interesting in view of the recent developments in organic and molecular electronics.[19] A conjugated oligomer (polymer)/nanocrystal hybrid can be considered as a molecular junction of two semiconductors of different electron-donating and electron-accepting properties or—if the conjugated oligomer (polymer) is doped—as a junction between a semiconductor and a metal. Such a molecular interface facilitates exciton dissociation and separation in organic solar cells, which as a consequence improves the device efficiency.[20] In this research we demonstrate that aniline tetramer can be grafted on CdSe nanocrystals using a carbodithioate-based bifunctional ligand. We have chosen aniline tetramer because it can be considered as a good model compound for polyaniline. Polyaniline and its oligomers show interesting nonlinear electrical transport properties in their undoped (semiconducting) state[21] and high electrical conductivity after doping.[22] These properties, combined with good stability, make the polyaniline family of organic conductors very important for future organic electronics development.

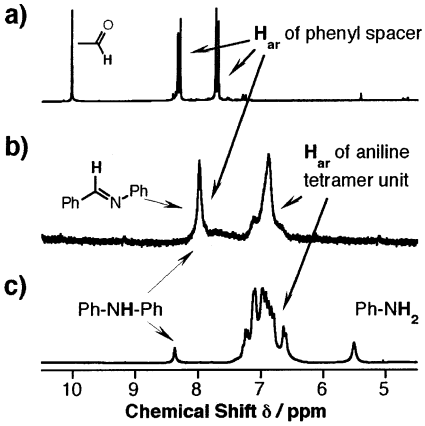

Figure 4. ^{1}H NMR spectra of (a) the bifunctional ligand **5′**, (b) CdSe nanocrystals after capping with ligand **5′** and grafting of aniline tetramer (**6**), resulting in **CdSe-8**, and (c) aniline tetramer (emeraldine base form) (**6**).

To facilitate possible charge transfer between the nanocrystal and the conjugated oligomer, we designed a bifunctional ligand with a conjugated spacer, 4-formyldithiobenzoic acid (**5**). The aldehyde group allows for the direct grafting of aniline tetramer via a condensation reaction with the amine group of the tetramer, during which an azomethine linkage is formed (see Scheme 1). During the ligand synthesis, the aldehyde group requires appropriate protection when introducing the carbodithioic acid anchoring group by Grignard reaction. Furthermore, deprotection in acidic conditions would be advantageous. Taking into account these restrictions, acetale formation by means of a diol turned out to be the most efficient protection method for the synthesis of **5**. After transformation into its salt form **5′**, the bifunctional ligand rapidly (within 1 h) and quasi-quantitatively (>95%) exchanges the initial TOPO ligands on the surface of CdSe nanocrystals. It should be emphasized that the use of ligand **5′** does not only permit the conjugation of aniline tetramer; in principle, any kind of primary amine can be grafted on the nanocrystal surface by this means.

The completeness of the grafting reaction is fully confirmed by the analysis of the ^{1}H NMR spectra of both reagents and the product (Figure 4). First, we notice that the peak at 10.0 ppm, characteristic of the aldehyde group in potassium

(19) (a) Katz, H. E.; Bao, Z.; Gilat, S. L. *Acc. Chem. Res.* **2001**, *34*, 359−369. (b) Dimitrakopoulos, C. D.; Malenfant, P. R. L. *Adv. Mater.* **2002**, *14*, 99−117.
(20) Brabec, C. J.; Sariciftci, N. S.; Hummelen, J. C. *Adv. Funct. Mater.* **2001**, *11*, 15−26.
(21) Kieffel, Y.; Travers, J.-P.; Ermolieff, A.; Rouchon, D. *J. Appl. Polym. Sci.* **2002**, *86*, 395−404.
(22) (a) Cao, Y.; Smith, P.; Heeger, A. J. *Synth. Met.* **1992**, *48*, 91−97. (b) Adams, P. N.; Devasagayam, P.; Pomfret, S. J.; Abell, L.; Monkman, A. *J. Phys. Condens. Matter.* **1998**, *10*, 8293−8303.

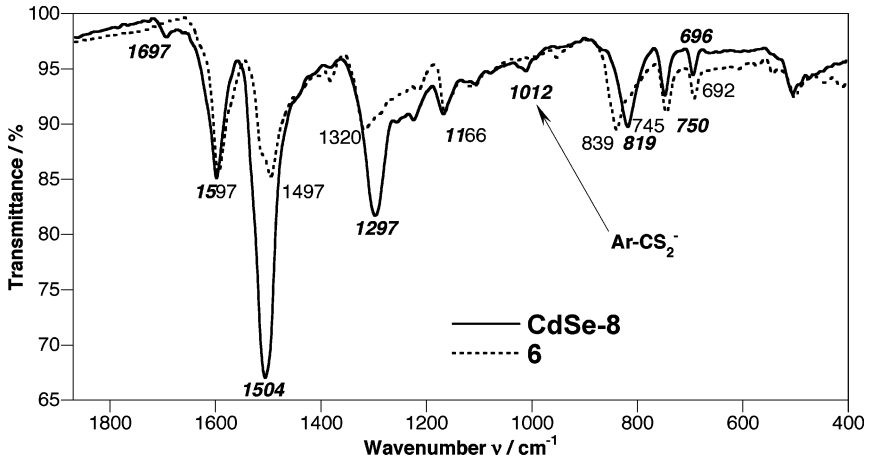

Figure 5. FT-IR spectra of aniline tetramer (**6**) and of CdSe nanocrystals after grafting of **6**, resulting in **CdSe-8**.

4-formyldithiobenzoate (**5′**), completely disappears. The same applies to the line at 5.5 ppm ascribed to the protons of the terminal amine group of "free", nongrafted, aniline tetramer. The spectrum of the condensation reaction product consists of two sets of broad, poorly resolved lines. This broadening is a simple consequence of the restricted rotation of the grafted organic molecules on the nanocrystal surface.[11a] The set of lines at ca. 8 ppm comprises the contribution from the aromatic protons of the phenyl group in ligand **5′** and the contribution from the amine protons of the aniline tetramer, as well as the contribution from the proton of the azomethine group. The second set of broad peaks, between 6.6 and 7.2 ppm, corresponds to the aromatic protons of the aniline tetramer.

Additional insight into the grafting reaction can be extracted from the IR spectra of the "free" aniline tetramer (**6**) and the nanocrystal−tetramer hybrid, **CdSe-8** (Figure 5). Consistent with the ^{1}H NMR data, the band at 1697 cm^{-1} in the spectrum of the hybrid, which originates from the C═O stretchings in the aldehyde group, is very weak, indicating that aniline tetramer is grafted on almost all aldehyde functions on the surface, i.e., that the grafting process is essentially quantitative. Additionally, a band at 1012 cm^{-1}, ascribed to the aromatic carbodithioate group,[23] appears upon grafting. All bands attributed to phenylene/phenyl rings vibrations[24] increase in intensity upon grafting. This is partially a consequence of the fact that the ratio of benzoid to quinoid rings increases in the nanocrystal−tetramer hybrid as compared to the "free" tetramer, due to the phenyl ring in ligand **5′**. Consistent with the grafting via the primary amine group, its characteristic band at 1380 cm^{-1}, present in the "free" tetramer spectrum, is absent in the spectrum of the hybrid. The band characteristic of the C═N stretchings in the azomethine group, usually located in the vicinity of 1600−1620 cm^{-1}, is obscured by the strong band at 1597 cm^{-1} originating from the C═C stretchings in the quinoid ring,[23] and is present as a shoulder. Note also small grafting-induced shifts of bands attributed to phenylene/phenyl C−H out-of-plane deformations in the 840−690 cm^{-1} spectral region.

Since **CdSe-8** can be considered as an adduct of two chromophores of different nature, it is worthwhile to analyze its UV−vis spectrum with the emphasis on grafting-induced spectral changes. The UV−vis spectrum of the "free" tetramer **6**, recorded in DMSO (see Figure 6), consists of two bands at 306 and 591 nm, which are ascribed to the $\pi-\pi^*$ transition in the benzene ring and to an excitonic-type transition between the HOMO level of the quinone ring and the LUMO level of the benzene ring, respectively.[25] The presence of the latter band confirms that the tetramer is in the oxidation state of emeraldine base. The positions of both bands are very sensitive to the extent of conjugation, being bathochromically shifted for oligomers with increasing chain length.[26] If we compare this spectrum with the one recorded for **CdSe-8**, we first notice that it is fully dominated by the absorption bands originating from the tetramer part. This is not unexpected, taking into consideration the rather high value of the molar absorption coefficient of the oligomer. Second, both absorption bands are bathochromically shifted by 19 and 27 nm, respectively. The band originating from the excitonic transition decreases in intensity with respect to the $\pi-\pi^*$ transition band and slightly broadens. These changes manifest a decreasing contribution of the quinoid structure and an increasing conjugation length in the grafted tetramer, which now extends to the phenyl ring, originating from ligand **5′**, via the azomethine link (see Scheme 1). To prove this hypothesis, we have synthesized model compound **7** by a condensation reaction between aniline tetramer and *p*-bromobenzaldehyde. Apart from the carbodithioate group, this molecule is identical to the organic moiety grafted on the nanocrystal surface in **CdSe-8** (see Scheme 1). Its spectrum is very similar to that recorded for **CdSe-8**, which unequivocally indicates the extended conjugation (Figure 6). As already discussed above, the carbodithioate ligand has an absorption band in the spectral region of the band characteristic of the $\pi-\pi^*$ transition in the grafted tetramer. This band, being bathochromically shifted upon the grafting reaction to CdSe nanocrystals, strongly overlaps with the $\pi-\pi^*$ transition band and causes an apparent increase of the $\pi-\pi^*$ transition band intensity in **CdSe-8** as compared to **7**.

Finally, we have carried out PL measurements in order to identify possible charge or excitation transfer between the nanocrystal and the electroactive capping molecules. Significant

(23) (a) Gotthardt, H.; Pflaumbaum, W.; Gutowski, P. *Chem. Ber.* **1988**, *121*, 313−322. (b) Gade, T.; Streek, M.; Voss, J. *Chem. Ber.* **1988**, *121*, 2245−2249.
(24) Boyer, M. I.; Quillard, S.; Louarn, G.; Lefrant, S. *Synth. Met.* **1999**, *101*, 782−783.
(25) Zheng, W.; Angelopulos, M.; Epstein, A. J.; MacDiarmid, A. J. *Macromolecules* **1997**, *30*, 7634−7637.
(26) Boyer, M.; Quillard, S.; Cochet, M.; Lourn, G.; Lefrant, S. *Electrochim. Acta* **1999**, *44*, 1981−1987.

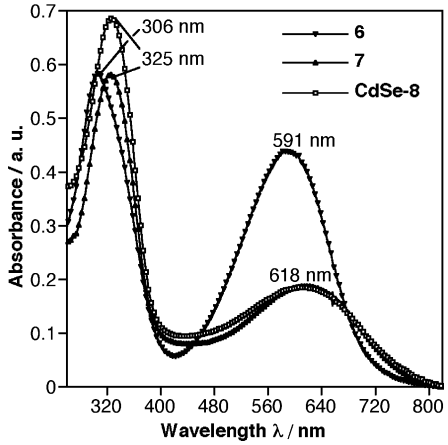

Figure 6. UV−vis absorption spectra of aniline tetramer (**6**), of CdSe nanocrystals after grafting of aniline tetramer (**CdSe-8**), and of the model compound **7**.

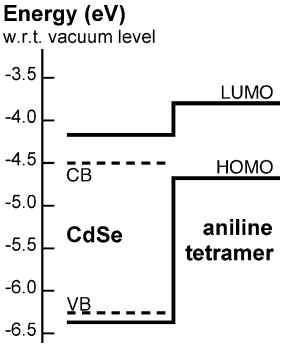

Figure 7. Electronic energy level alignment for bulk CdSe (dashed lines), 4.2-nm-diameter CdSe nanocrystals, and aniline tetramer (full lines).[27] The energy shift due to the quantum confinement in the nanocrystals is shared between the electron (conduction band) and hole (valence band) states with a 3:1 ratio, taking the electron affinity of bulk CdSe as 4.5 eV.[29]

changes in the fluorescence properties of the newly synthesized hybrid are expected because of the relative positions of the nanocrystal and ligand electronic levels, depicted in Figure 7. This scheme is constructed assuming the electron affinity of the nanocrystals to be 4.2 eV (diameter 4.2 nm, gap 2.2 eV),[27] and the HOMO level of aniline tetramer in the oxidation state of emeraldine base to be 4.7 eV.[28] Once an electron−hole pair is excited in the system, the electron should relax to the lower energy state located on the nanocrystal, while the hole should relax toward states located on the aniline tetramer. The hybrid compound should thus provide a very efficient separation of charges, resulting in PL quenching.

The hypothesis outlined above is corroborated by the PL spectra presented in Figure 8. The spectrum of TOPO-capped CdSe nanocrystals is characterized by a narrow emission peak centered at 575 nm. The ligand exchange leading to **CdSe-5′** results in a total extinction of this PL. We explain that by a charge transfer from the nanocrystal to the ligand aromatic ring, which inhibits the radiative recombination of the excitons photocreated on the nanocrystal. On the other hand, the

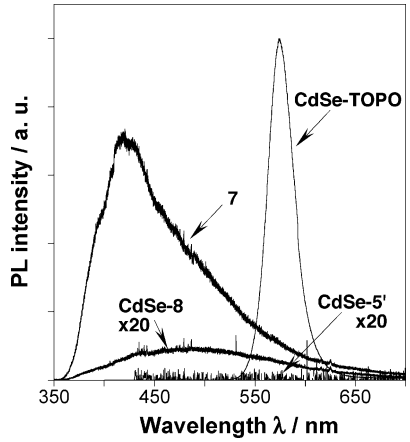

Figure 8. PL spectra of TOPO-capped CdSe nanocrystals, of model compound **7**, as well as of 4-formyldithiobenzoate-capped nanocrystals before (**CdSe-5′**) and after (**CdSe-8**) grafting of aniline tetramer (excitation wavelength 365 nm). The TOPO-capped CdSe nanocrystals' spectrum has been downscaled in order to fit to the same graph.

conjugated model compound **7,** which, apart from its terminal group, can be considered as an adduct of the ligand **5′** and the aniline tetramer **6**, gives rise to a large emission band between 350 and 600 nm. This is essentially the same as the PL of the aniline tetramer, which can be expected due to the structural similarity between the two molecules. Finally, **CdSe-8** shows a nearly complete extinction of the PL of both the nanocrystal and organic moieties. The arguments based on the relative positions of the electronic energy levels apply as above: excitation of the nanocrystal can lead to the transfer of holes toward the oligomeric ligand, while excitation of the latter can result in the transfer of electrons onto the nanocrystal. Further experiments, namely PL excitation spectroscopy, are underway in order to identify the location of the absorbing levels in the newly synthesized hybrid compound.

Conclusion

To summarize, we have demonstrated that carbodithioic acids and their salts, never previously used for the functionalization of CdSe nanocrystals, provide a facile and quasi-quantitative exchange with original nanocrystal surface ligands (TOPO). Moreover, because of the formation of strong chelate-type bonding with the metal atoms at the nanocrystal surface, carbodithioates significantly improve nanocrystals' stability against photooxidation. Finally, a simple synthesis method allows for the integration of functional groups, offers high flexibility in the design of new ligands, and facilitates the grafting of other molecules and macromolecules, such as conjugated oligomers or polymers. We strongly believe that the use of carbodithioic acids and their derivatives is by no way restricted to the functionalization of CdSe nanocrystals but can be extended to other types of semiconductor and metal nanocrystals as well as to core/shell systems. The synthesis of a new carbodithioate ligand permitting the hydro-solubilization of highly luminescent core/shell nanocrystals is underway.

Acknowledgment. The authors thank Dr. B. Dufour and Dr. P. Rannou for providing a sample of aniline tetramer, as well as Dr. N. Charvet for helpful discussions.

JA047882C

(27) Greenham, N. C.; Peng, X.; Alivisatos, A. P. *Phys. Rev. B* **1996**, *54*, 17628−17637.
(28) Libert, J.; Cornil, J.; dos Santos, D. A.; Brédas, J. L. *Phys. Rev. B* **1997**, *56*, 8638−8650.
(29) Chiang, T. C.; Himpsel, F. J. *Electronic Structure of Solids*; Landolt-Börnstein, New Series, Group III, Vol. 23, Pt. 2; Springer: Berlin, 1989.